

# Development of a portable wrist MRI for skeletal age assessment

Yasuhiko Terada<sup>1</sup>, Kazunori Ishizawa<sup>1</sup>, Shinya Inamura<sup>1</sup>, and Katsumi Kose<sup>1</sup>

<sup>1</sup>Institute of Applied Physics, University of Tsukuba, Tsukuba, Ibaraki, Japan

## INTRODUCTION

MR imaging of hand and wrist is beneficial in assessment of maturity and growth for children [1,2]. Having a portable wrist MRI system enables skeletal age assessment in remote place, which can provide a chance for many children to have an examination in a less stressful environment. However, there is no such a portable scanner that provides 3D images with a large FOV necessary for skeletal age assessment. The MagneVu with a permanent 0.2 T magnet [3] is a portable extremity scanner, but it is unfit for skeletal assessment because of its reduced FOV and poor spatial resolution. Here, we develop a portable wrist scanner with a small permanent magnet (135 kg in weight) that allows 3D imaging in a large volume ( $8 \times 8 \times 4 \text{ cm}^3$  diameter ellipsoidal volume (DEV)) without special RF shielding. With optimized gradient coils and an RF probe, the new system provides high quality images that are as reliable as those provided by a conventional compact hand MRI system (with a 700 kg magnet) [4].

## MATERIALS AND METHODS

A portable system consisted of a C-type Nd-Fe-B permanent magnet (Neomax Engineering, Tokyo, Japan; field strength = 0.306 T, gap width = 8 cm, sizes =  $27 \times 39.2 \times 31 \text{ cm}^3$ , weight = 135 kg, and homogeneity = 8.5 ppm over  $8 \times 8 \times 4 \text{ cm}^3$  DEV) (Fig. 1(a) and Table 1), an RF probe (Fig. 2), a gradient coil set (Fig. 3), and an MRI console. The RF coil (10 turn; 9 cm long) was designed as a set of stacked current loops with spacing optimized using a particle swarm optimization algorithm to maximize  $B_1$  homogeneity. The RF coil was made by winding Cu foil (0.1 mm thick; 7 mm width) around an oval acrylic pipe (aperture:  $10 \text{ cm} \times 4.7 \text{ cm}$ ; length = 16 cm). The RF coil was shielded by an RF probe box made of 0.3-mm-thick brass plates. A 5-mm-thick aluminum plate was connected to the brass box to ground the arm to minimize interference by external RF noise. The  $x$ - and  $y$ -gradient coils were designed as a combination of a circular arc and third-order Bezier curve with the position and center angle optimized using an artificial bee colony (ABC). The  $z$ -gradient coil was designed as a combination of circular current loops with diameter optimized using an ABC. In each calculation, the coil pattern was restricted to a circular region (10 cm in diameter). Each gradient coil element was made by winding polyethylene-coated Cu wire (0.6 mm in diameter) on a surface of fiber-reinforced plastic (FRP) plate (24 cm in diameter; 0.5 mm thick) and tracing a printed coil pattern attached on the other side of the plate.  $x$ ,  $y$ , and  $z$  coil elements were then stacked together using epoxy resin.

A regularly-spaced lattice phantom was imaged using a 3D spin echo sequence (TR/TE = 80/20ms; FOV =  $10 \times 10 \times 10 \text{ cm}^3$ ; matrix size =  $256 \times 128 \times 128$ ; pixel bandwidth = 97.7 Hz) to evaluate image distortion due to  $B_0$  inhomogeneity and gradient nonlinearity. The left wrist of a healthy female volunteer aged 22 was imaged to evaluate image quality using a 3D coherent gradient echo sequence (TR/TE = 40/11ms; FA = 60; FOV =  $10 \times 10 \times 5 \text{ cm}^3$ ; matrix size =  $256 \times 128 \times 32$ ; pixel bandwidth = 97.7 Hz). The wrist image was compared with that provided by a conventional hand scanner with a 0.3 T permanent magnet [2,4] (FOV =  $20 \times 10 \times 5 \text{ cm}^3$ ; matrix size =  $512 \times 128 \times 32$ ; and other parameters were the same as above).

## RESULTS

Table 1 summarizes the measured values of  $B_0$  and  $B_1$  inhomogeneities, gradient nonlinearity, and gradient efficiency. Figure 3(c) shows a center slice of 3D MR images of a lattice phantom. Figure 4 shows coronal sections of the left wrist obtained using the portable and conventional hand scanners. In Fig. 4(b), the upper half area was trimmed away to equalize the imaging areas.

## DISCUSSION

The magnet is light (135 kg) and readily portable by four people. The 5 gauss line is only 50 cm apart from the magnet center, and the system requires no shield room. Thus, the system can be placed anywhere. Despite the small magnet gap (8 cm), the  $B_0$  homogeneity and gradient linearity were high (Fig. 1(b) and Table 1) over a large area ( $8 \times 8 \times 4 \text{ cm}^3$  DEV) covering the whole wrist and carpal bones. This permits imaging with less distortion, as shown in Fig. 3(c). The high homogeneities of  $B_0$  and  $B_1$  allowed high signal uniformity. The image signal-to-noise ratio (SNR) was comparable to that obtained using the conventional hand scanner. The image quality of the wrist was high enough to resolve anatomical structures of bones, which is necessary for skeletal age assessment.

In conclusion, we developed the portable wrist MRI system which provides high quality images comparable to those provide by the conventional hand scanner.

**REFERENCES:** [1] J. Dvorak et al., Age determination by magnetic resonance imaging of the wrist in adolescent male football players, *Br. J. Sports Med.* **41** 45 (2006). [2] Y. Terada et al., Skeletal age assessment in children using an open compact MRI system, *Magn. Reson. Med.* (2012). doi: 10.1002/mrm.24439. [3] G. Gold et al., MR imaging of the wrist with a portable extremity scanner, *ISMRM Proc.* 2039 (1999). [4] S. Handa et al., Development of a local electromagnetic shielding for an extremity magnetic resonance imaging system, *Rev. Sci. Instrum.* **79**, 113706 (2008).

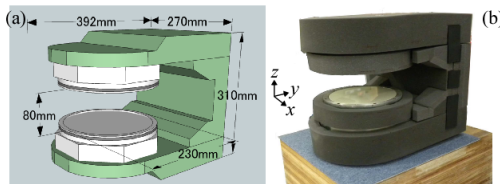


Fig. 1: (a) 0.3 T permanent magnetic circuit. (b)  $\Delta B_0$  map in  $8 \times 8 \times 4 \text{ cm}^3$  DEV.

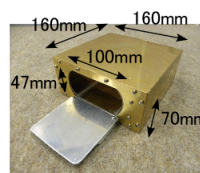


Fig. 2: RF probe

Magnet weight	135 kg	
Magnet size	270 mm x 392 mm x 310 mm	
Magnet gap	8 cm	
Center Larmor frequency	13.0 MHz (0.306 T)	
Inhomogeneities over $8 \times 8 \times 4 \text{ cm}^3$ DEV	$B_0$	8.5 ppm (RMS), 83 ppm (PP)
	$B_1$	20 % (RMS)

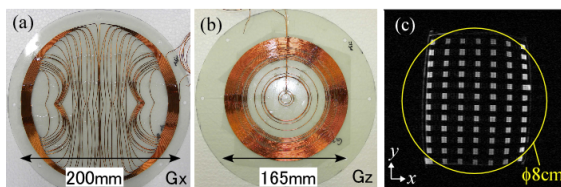


Fig. 3: (a), (b) Gradient coils (a)  $G_x$  and (b)  $G_z$ . (c) MR image (center slice) of a regularly-spaced lattice phantom.

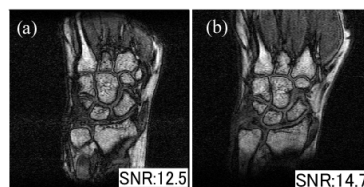


Fig. 4: MR images of a wrist obtained using (a) the portable and (b) the conventional hand scanners. In (b), the upper half area was trimmed away to equalize the imaging areas.

Gradient properties	$G_x$	$G_y$	$G_z$
Nonlinearity over $8 \times 8 \times 4 \text{ cm}^3$ DEV	7%	7%	6%
Efficiency [ $\times 10^{-3} \text{ T/m/A}$ ]	7.4	7.3	1.6
Gradient coil gap	76 mm	77.5 mm	79 mm

Table 1: Properties of constructed system. RMS and PP represent root mean square and peak-to-peak, respectively.